

1 **Supplementary information**

2

3 **Supplementary figure and movie legends**

4 **Supplementary Figure 1. Various membrane damaging agents induce ESCRT proteins**
5 **recruitment to the site of rupture.** *D. discoideum* expressing GFP-Vps32 or Vps4-GFP were treated
6 with digitonin, GPN, LLOMe, purified recombinant ESAT-6 or medium (control) and visualized over
7 time. Still images show representative cells in phase-contrast and fluorescence at 0, 5, 10 and 15 min
8 after treatment. On the right, magnification of one of the images per treatment. Red arrows point to GFP-
9 Vps32 and Vps4-GFP structures at the sites of damage. Scale bars 10 μ m.

10

11 **Supplementary Figure 2. Spatial association of GFP-Vps32 with damaged lysosomes.** *D.*
12 *discoideum* expressing GFP-Vps32 were incubated with TRITC-Dextran (red) (A) or Alexa Fluor 647
13 Dextran (red) (B) for at least 3 h to label all endosomes, treated with LLOMe or GPN, respectively, and
14 monitored by time-lapse microscopy. Kymographs generated by a repeated linescan through a
15 representative cell show the sustained association of GFP-Vps32 structures with the lysosomes and
16 endosomes (black and white arrows). In B, the compound was added immediately before imaging
17 started.

18

19 **Supplementary Figure 3. Ultrastructural appearance of the escape site of *M. marinum* in several**
20 **ESCRT mutants.** *D. discoideum* were infected with *M. marinum* and fixed for TEM at 24 hpi. *M.*
21 *marinum* ("*M.m.*" labelled in red) accessed the cytosol in wt (A and D), *tsg101*- (B and C), *alix*- (E) and
22 *alg2a-/b-* (F). Sites of membrane disruption are highlighted with blue arrows. (C) High magnification
23 inset of the region of interest in (B). Scale bars, 1 μ m.

24

25 **Supplementary Figure 4. Ubiquitination and GFP-Plin recruitment as readout of *M. marinum***
26 **cytosolic access.** (A-B) *D. discoideum* wt or mutant (*atg1*-, *tsg101*- or *atg1-tsg101*-) were fixed for
27 immunofluorescence. Post-lysosomes were labelled with p80 (green), nuclei were labelled with DAPI
28 (blue), ubiquitin was in green and Atg8 in red. (C-D) *D. discoideum* wt or mutant (*atg1*-, *tsg101*-, or
29 *atg1-tsg101*-) were infected with *M. marinum* (blue) and fixed for immunofluorescence. Both

30 ubiquitin and Atg8 (green) decorated the bacteria when the MCV (p80, red) was disrupted. Scale bars
31 1 μm . (E) *D. discoideum* wt or mutant (*atg1-*, *tsg101-*, or *atg1-tsg101-*) expressing GFP-Plin (green)
32 were infected with *M. marinum* for live microscopy. All mutants showed an increase of GFP-Plin
33 recruitment on the bacteria (red). (F) Proportion of the *M. marinum* bacteria or microcolonies decorated
34 with GFP-Plin. The plot shows the mean and standard deviation (WT N=4, n=139; *atg1-* N=3, n=148;
35 *tsg101-* N=3, n=98; *atg1-tsg101-* N=3, n=191). Two-tailed *t*-tests were performed.

36

37 **Supplementary Figure 5. AlxA and Alg2a/b do not impact *M. marinum* intracellular replication.**

38 (A) *D. discoideum* wt or mutant (*alxA-* or *alg2-/b-*) were infected with *M. marinum* and fixed for
39 immunostaining at 8 hpi (*M. marinum* in red, ubiquitin in green, DAPI in blue). Arrows point to
40 ubiquitinated bacteria. Scale bars, 10 μm and 5 μm for the insets. (B) Quantification of the proportion
41 of ubiquitinated bacteria or bacterial microcolonies. The plot shows the mean and standard deviation
42 [WT (JH10) N=4, n=144; *alxA-* (JH10) N=3, n=134; *alg2a-/b-* (JH10) N=3, n=266]. (C) *D.*
43 *discoideum* wt or mutant (*alxA-* or *alg2-/b-*) were infected with *M. marinum* and fixed for
44 immunostaining at 8 hpi (*M. marinum* in red, Atg8 in green, DAPI in blue). Arrows point to bacteria
45 decorated with Atg8. Scale bars, 10 μm and 5 μm for the insets. (D) Quantification of the proportion of
46 bacteria or bacterial microcolonies decorated with Atg8. The plot shows the mean and standard deviation
47 [WT (JH10) N=4, n=275; *alxA-* (JH10) N=4, n=170; *alg2a-/b-* (JH10) N=4, n=448]. Two-tailed
48 *t*-test were performed. (E-F) *D. discoideum* wt or mutant (*alxA-* or *alg2-/b-*) were infected with *M.*
49 *marinum* (blue) and fixed for immunofluorescence. Both ubiquitin and Atg8 (green) decorate the
50 bacteria when the MCV (p80, red) was disrupted. Scale bars, 1 μm . (G-H) *D. discoideum* wt or mutant
51 (*alxA-* or *alg2-/b-*) were infected with luminescent *M. marinum* and intracellular bacterial growth was
52 monitored in a plate reader over 72 hpi. There was no significant difference between *M. marinum* growth
53 in wt and mutants. Plots represent the mean and standard deviation of N=3 independent experiments.
54 Two-way ANOVA was performed.

55

56

57

58 **Supplementary Movie 1. The ultrastructure of the MCV at the site of *M. marinum* escape.** FIB-
59 SEM stack and corresponding 3D reconstruction of the damaged MCV shown in Fig. 1D. “*M.m.*”,
60 *Mycobacterium marinum* (in dark blue); “MCV”, *Mycobacterium*-containing vacuole (in light blue);
61 electron-dense material surrounding the cytosolic bacteria, in yellow.

62
63 **Supplementary Movie 2. GFP-Vps32 forms rings in the vicinity of *M. marinum*.** Time-lapse of a *D.*
64 *discoideum* cell expressing GFP-Vps32 and infected with *M. marinum* wt (red). Arrows show GFP-
65 Vps32 rings which formed and seemed to move along the bacterium. Scale bar, 10 μ m.

66
67 **Supplementary Movie 3. Dynamics of GFP-Vps32 recruitment in the vicinity of the MCV.** Time-
68 lapse of a *D. discoideum* cell expressing GFP-Vps32 and AmtA-mCherry and infected with *M. marinum*
69 wt (red). Scale bars, 10 μ m.

70
71 **Supplementary Movie 4. Localisation of ESCRT and autophagy components upon digitonin**
72 **treatment.** Time-lapse imaging of *D. discoideum* cells expressing GFP-Tsg101, GFP-Vps32, Vps4-
73 GFP or GFP-Atg8 upon digitonin treatment. Scale bar, 10 μ m.

74
75 **Supplementary Movie 5. Localisation of ESCRT and autophagy components upon LLOMe**
76 **treatment.** Time-lapse imaging of *D. discoideum* cells expressing GFP-Tsg101, GFP-Vps32, Vps4-
77 GFP or GFP-Atg8 upon LLOMe treatment. Cells were incubated with fluorescent dextran (red) for at
78 least 3 h prior to the treatment. Scale bar, 10 μ m.

79
80 **Supplementary Movie 6. Annexin V labels membrane damage upon digitonin treatment.** Time-
81 lapse imaging of *D. discoideum* cells that were incubated with Annexin V Alexa Fluor 594 conjugate in
82 the presence of Ca^{2+} and then treated with digitonin. Arrowheads point to the site of membrane
83 disruption. Scale bar, 10 μ m.

84
85 **Supplementary Movie 7. Related to Figure 5G and Figure 5H. Lysosomal leakage upon LLOMe**
86 **treatment.** Time-lapse imaging of *D. discoideum* wt, *tsg101*- and *atg1*- that were incubated with the 10
87 kDa Alexa Fluor 647 dextran (red) and the 0.5 kDa soluble pH indicator HPTS (green) and then treated
88 with LLOMe. Scale bar, 10 μ m.

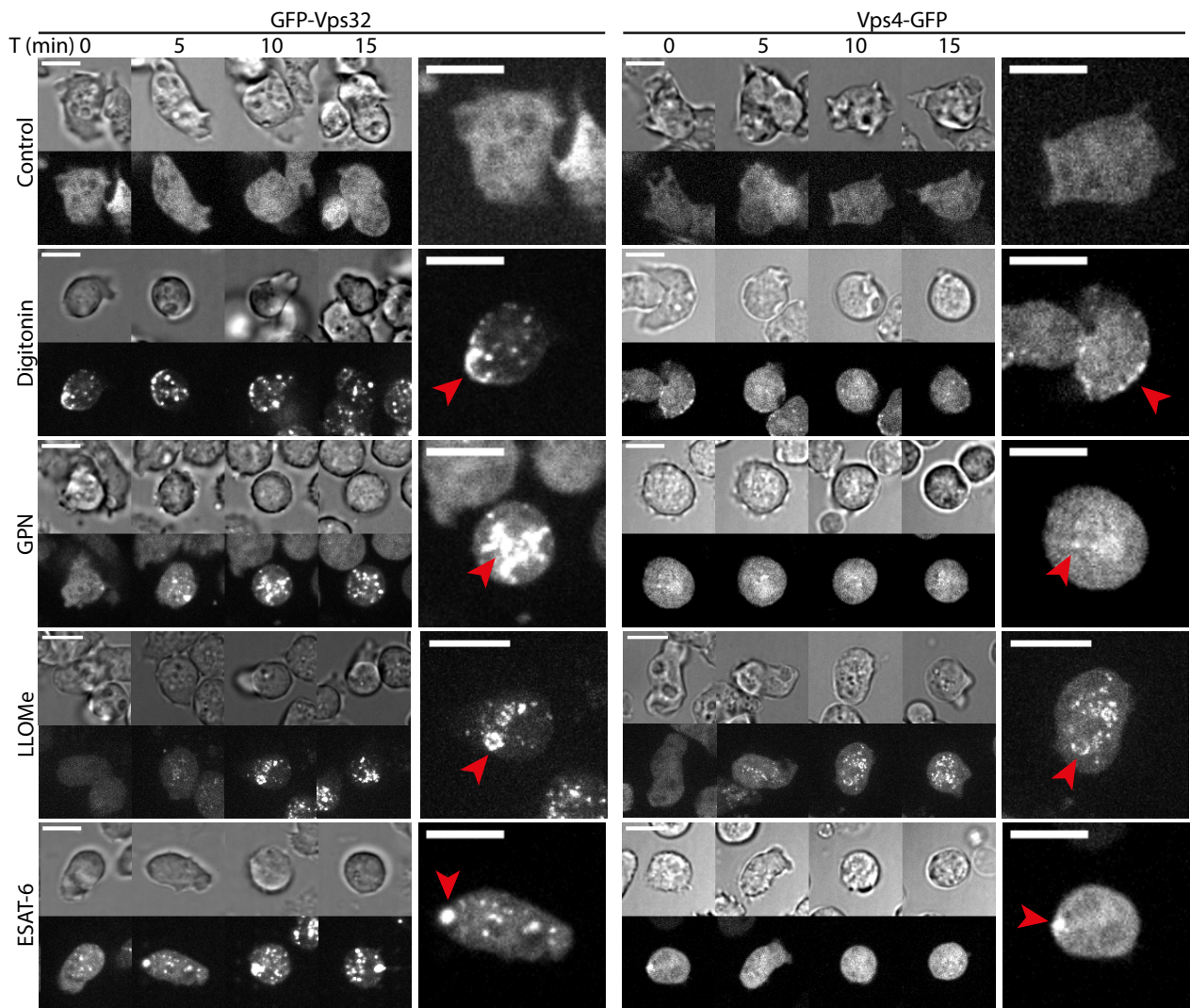
89 **Supplementary references**

- 90 1. Cardenal-Munoz E, *et al.* Mycobacterium marinum antagonistically induces an autophagic
91 response while repressing the autophagic flux in a TORC1- and ESX-1-dependent manner. *PLoS*
92 *Pathog* **13**, e1006344 (2017).
- 93 2. Mattei S, *et al.* Dd-Alix, a conserved endosome-associated protein, controls Dictyostelium
94 development. *Dev Biol* **279**, 99-113 (2005).
- 95 3. Aubry L, *et al.* Biochemical characterization of two analogues of the apoptosis-linked gene 2
96 protein in Dictyostelium discoideum and interaction with a physiological partner in mammals,
97 murine Alix. *J Biol Chem* **277**, 21947-21954 (2002).
- 98 4. Veltman DM, Akar G, Bosgraaf L, Van Haastert PJ. A new set of small, extrachromosomal
99 expression vectors for Dictyostelium discoideum. *Plasmid* **61**, 110-118 (2009).
- 100 5. King JS, Veltman DM, Insall RH. The induction of autophagy by mechanical stress. *Autophagy* **7**,
101 1490-1499 (2011).
- 102 6. Du X, *et al.* Dictyostelium lipid droplets host novel proteins. *Eukaryot Cell* **12**, 1517-1529 (2013).
- 103 7. Barisch C, Paschke P, Hagedorn M, Maniak M, Soldati T. Lipid droplet dynamics at early stages
104 of Mycobacterium marinum infection in Dictyostelium. *Cell Microbiol* **17**, 1332-1349 (2015).
- 105 8. Carroll P, *et al.* Sensitive detection of gene expression in mycobacteria under replicating and non-
106 replicating conditions using optimized far-red reporters. *PLoS One* **5**, e9823 (2010).
- 107 9. Andreu N, *et al.* Optimisation of bioluminescent reporters for use with mycobacteria. *PLoS One* **5**,
108 e10777 (2010).

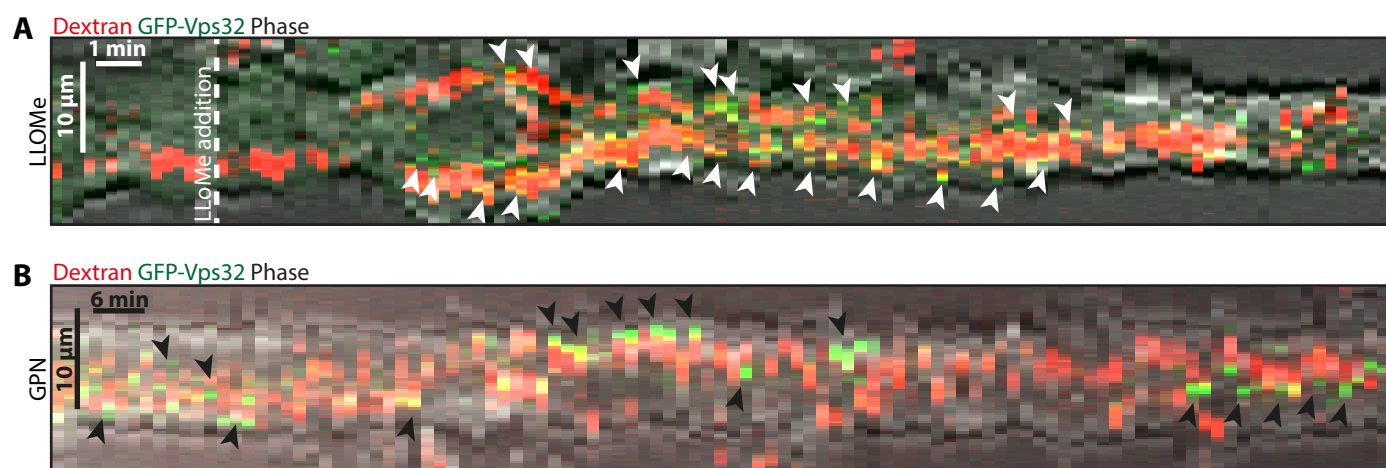
109

110

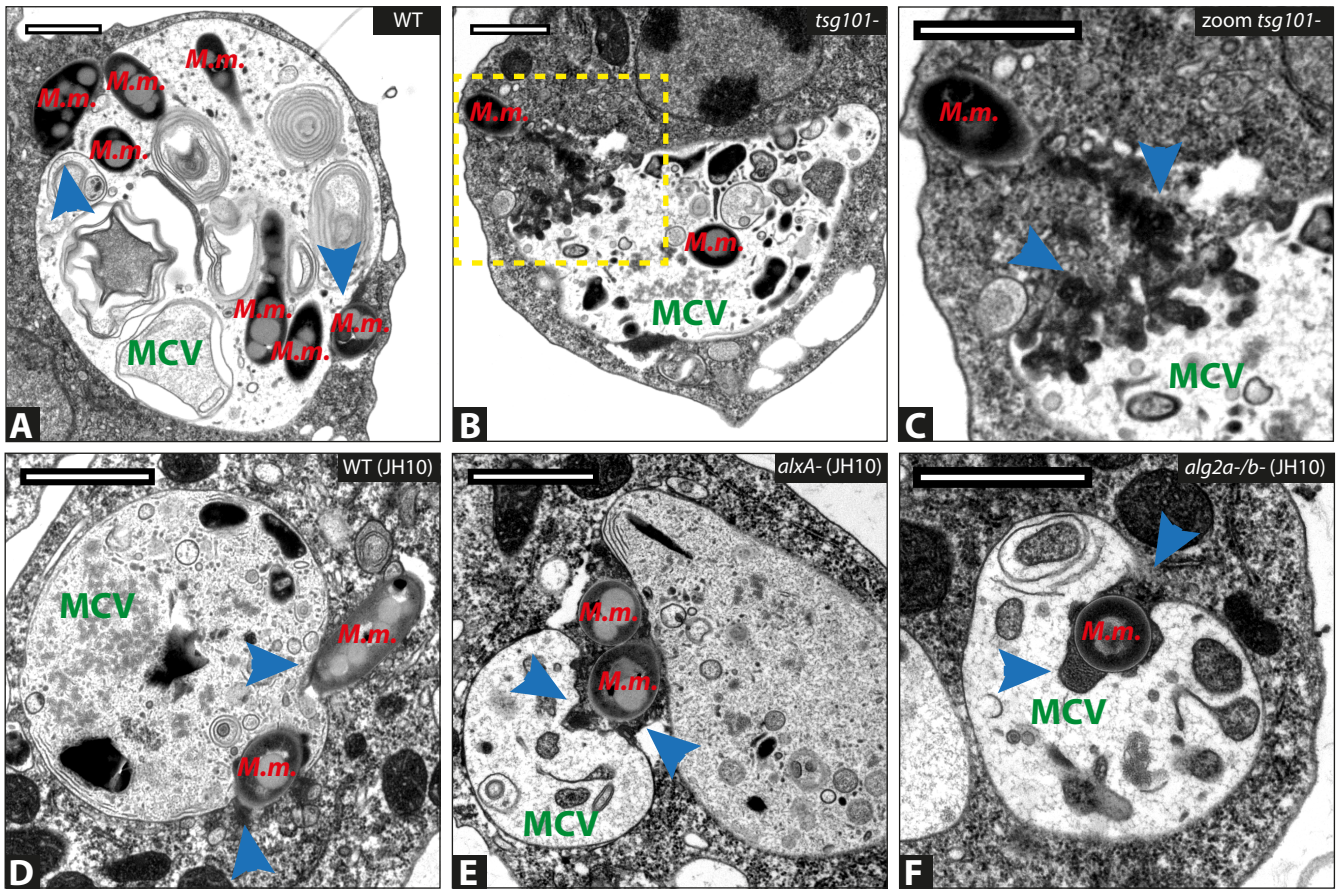
Supplementary Figure 1



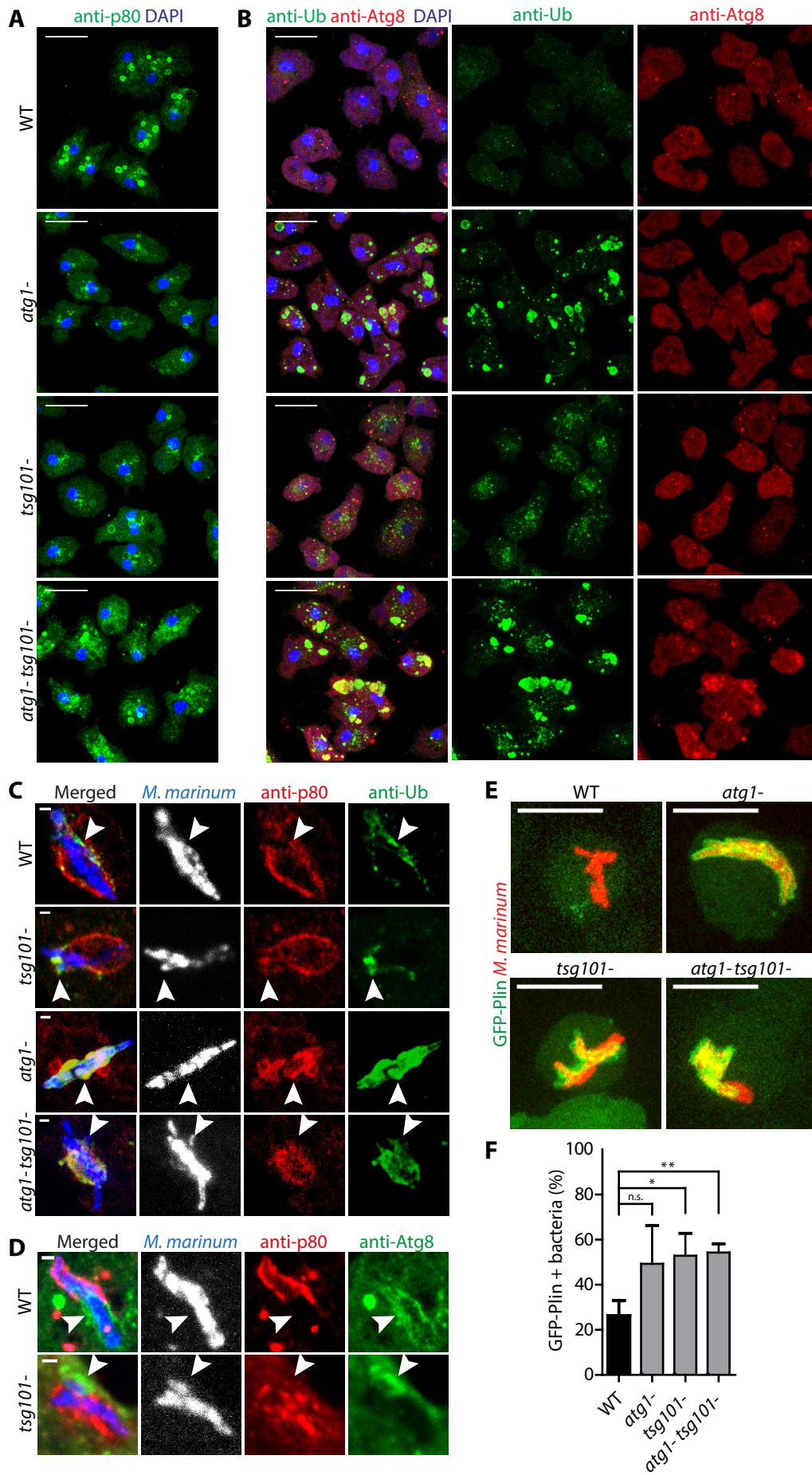
Supplementary Figure 2



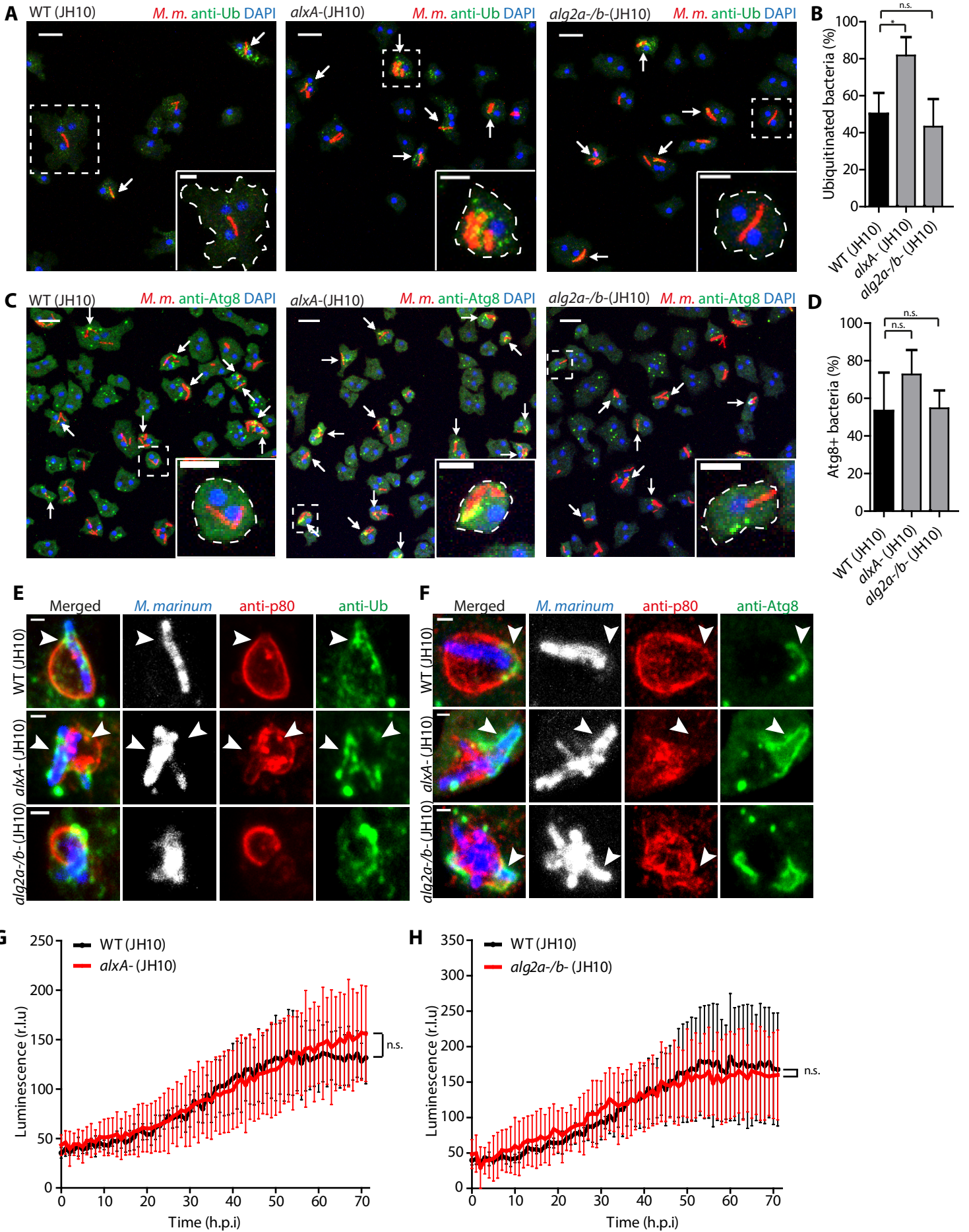
Supplementary Figure 3



Supplementary Figure 4



Supplementary Figure 5



111 **Supplementary Table 1.**

112

Strain/Plasmid	Relevant characteristics	Source/Reference
<i>D. discoideum</i>		
Ax2(Ka)	wt	
JH10	wt	
Ax2(Ka) <i>atg1</i> -	KO	1
Ax2(Ka) <i>tsg101</i> -	KO	This study
Ax2(Ka) <i>atg1</i> - <i>tsg101</i> -	KO	This study
JH10 <i>alxA</i> -	KO	2
JH10 <i>alg2a/b</i> -	KO	3
<i>M. marinum</i>		
M strain	wt	L. Ramakrishnan (Washington University)
ΔRD1	KO	L. Ramakrishnan (Washington University)
<i>D. discoideum</i> plasmids		
pDM317		4
pDM323		1
pJSK500	GFP-Atg8a	5
GFP-Tsg101	<i>tsg101</i> cDNA (DDB_G0286797) in pDM317	This study
GFP-Vps32	<i>vps32</i> cDNA (DDB_G0275573) in pDM317	This study
Vps4-GFP	<i>vps4</i> cDNA (DDB_G0284347) in pDM323	This study
pDNeoGFP-Plin	GFP-Plin	6
AmtA-mCherry	<i>amtA</i> cDNA(DDB_G0277503) in pDM1044	7
Mycobacteria plasmids		
pCherry10	mCherry under control of the G13 promoter, Hyg ^r	8
pMV306:: <i>lux</i>	bacterial luciferase under control of the G13 promoter, Kan ^r	9

113

114

115